energies

MDPI

Article

Parameter Estimation of Three Diode Photovoltaic Model Using Grasshopper Optimization Algorithm

Omnia S. Elazab [1], Hany M. Hasanien [1], Ibrahim Alsaidan [2], Almoataz Y. Abdelaziz [3] and S. M. Muyeen [4,*]

1 Electrical Power and Machines Department, Faculty of Engineering, Ain Shams University, Cairo 11517, Egypt; omniasolimanelazab@gmail.com (O.S.E.); hanyhasanien@ieee.org (H.M.H.)
2 Department of Electrical Engineering, College of Engineering, Qassim University, Buraydah 52571, Saudi Arabia; Alsaidan@qec.edu.sa
3 Faculty of Engineering and Technology, Future University in Egypt, Cairo 11835, Egypt; almoatazabdelaziz@hotmail.com
4 School of Electrical Engineering Computing and Mathematical Sciences, Curtin University, Perth, WA 6845, Australia
* Correspondence: sm.muyeen@curtin.edu.au

Received: 18 October 2019; Accepted: 17 January 2020; Published: 20 January 2020

Abstract: While addressing the issue of improving the performance of Photovoltaic (PV) systems, the simulation results are highly influenced by the PV model accuracy. Building the PV module mathematical model is based on its I-V characteristic, which is a highly nonlinear relationship. All the PV cells' data sheets do not provide full information about their parameters. This leads to a nonlinear mathematical model with several unknown parameters. This paper proposes a new application of the Grasshopper Optimization Algorithm (GOA) for parameter extraction of the three-diode PV model of a PV module. Two commercial PV modules, Kyocera KC200GT and Solarex MSX-60 PV cells are utilized in examining the GOA-based PV model. The simulation results are executed under various temperatures and irradiations. The proposed PV model is evaluated by comparing its results with the experimental results of these commercial PV modules. The efficiency of the GOA-based PV model is tested by making a fair comparison among its numerical results and other optimization method-based PV models. With the GOA, a precise three-diode PV model shall be established.

Keywords: optimization methods; photovoltaic power systems; power system modeling

1. Introduction

Solar energy is considered as a highly promising renewable energy resource [1]. For the 8th year now, solar power gained the largest share of innovative investments in renewable energies [2]. Driven by the International Governmental Support and the competition between the Photovoltaic (PV) manufacturers, PV modules with higher efficiencies and lower prices are released to the market. The global solar annual installed capacity exceeded 98 GW by the end of 2017 with expectations to reach 162 GW by 2021 [3,4]. An accurate simulation of a solar photovoltaic (PV) system is a prerequisite for actual implementation. Precise modeling of PV modules is the prime step for improving the performance of PV systems during simulation and design procedures. PV module is simulated by the I-V characteristic mathematical model. However, PV modeling is a complicated problem due to the nature of the I-V characteristic, which is a nonlinear relation that is highly affected with the variation of temperatures and solar irradiations [5–11].

The I-V mathematical model contains a large number of unknowns. The single and double diode model are the leading mathematical models for getting precise system modeling [12]. Single-Diode

model is characterized with its simplicity and a very acceptable degree of precision [13,14]. The output IV characteristic of single diode model can be modeled by identifying five unknown parameters, specifically, the PV current Ipv, diode saturation current I_0, ideality factor a, series resistance R_s, and parallel resistance R_p [15]. However, this model lacks precision at the open-circuit voltage at low irradiance as the carrier recombination losses in the depletion region are ignored [16,17]. The double diode model is introduced to overcome this problem. An extra diode is added to represent the recombination losses. The double-diode model shows more accuracy but that was on the account of a more complex model with a greater number of unknowns; an extra diode saturation current and its ideality factor of the second diode are added to the previous unknowns [17–19]. A better model with three diodes is introduced that addresses the effects of grain boundaries and leakage current [20]. Despite the ability of this model to meet most of physical requirements for the solar cell, it involves the calculation of nine parameters [21].

The parameter extraction is expressed as an optimization problem. The I-V characteristic equation is optimized by adjusting the previous unknown parameters. There are two approaches for solving this problem. They are assorted into mathematical optimization methods and stochastic optimization methods. Mathematical optimization uses numerical and analytical methods to solve the equations such as gradient-based information and curve fitting using Newton–Raphson algorithm [22]. Some of these methods suffer from complexity in arithmetic derivations, especially in double and triple diode models, so they acquire some assumptions and initial conditions [23]. Some approaches neglected the resistive effect, but their results were far away from accuracy [24,25]. Others assumed the equality of saturation currents in double diode model [26], while one of fundamentals is that I_{o2} is greater than I_{o1} [27]. That may lead to an inaccurate solution. They also may be trapped easily into a local optimum point and fail to reach the required global optimum for such highly nonlinear optimization problem [28].

Stochastic optimization is introduced to overcome these drawbacks. They depend on starting the optimization with random parameters in the search space to avoid being stuck in local optimum point [29]. Among stochastic optimization approaches, meta-heuristic algorithms are the most popular. They are classified into evolutionary and swarm intelligence algorithms. Evolutionary algorithms imitate the evolution principals in nature. Genetic algorithm (GA) is its most popular example. Swarm intelligence techniques imitate creatures that live in groups in nature. These techniques mimic the natural problems-solving thinking of these groups of creatures to reach their own main goal which is survival [30]. Recently, meta-heuristic techniques aided by artificial intelligence succeeded to solve the most complex, multi-variable problems. Many of the developed metaheuristic techniques are applied to the PV parameter extraction problem: Flower Pollination Algorithm (FPA) in [31] with the merit of independency on initial conditions; Shuffled Frog Leaping Algorithm (SFLA) in [14], which is characterized by the high convergence speed and Artificial Immune System (AIS) in [23], which focuses on the end goal.

A new nature-inspired metaheuristic technique known as Grasshopper Optimization Algorithm (GOA) is introduced in 2017 [32]. This technique is inspired from the way of grasshoppers in getting their food. Each grasshopper is randomly positioned in search space and moves within its boundaries with two types of movement. The life cycle of grasshoppers is divided into two stages, firstly it is a larva that moves slowly demonstrating exploitation and secondly it changes to an insect with dynamic movement that represents an exploration process [33]. The proposed GOA has been implemented in solving several mathematical functions and real problems applications [34,35]. The proposed algorithm solved the problems with a high accuracy. This algorithm managed to balance between exploitation and exploration processes reaching the global optimal point avoiding trapping into a local optima [32].

In this work, a novel appliance for the GOA is introduced to estimate the unknown parameters of the three-diode PV model of a PV module. The fitness function is evaluated by minimizing the root mean-square error between the calculated model current and its experimental value. The method is implemented as an objective function [36]. GOA-based PV models for both Kyocera KC200GT PV

module and Solarex MSX-60 PV modules are obtained. Using MATLAB program, simulations at various environmental conditions are carried out to validate the robustness of the models. The GOA-based PV models simulation results are compared with that determined by other metaheuristic optimization methods. The proposed PV model is evaluated by implementing a fair comparison between its results and the experimental results of these commercial PV modules. A comparison between the current error of the GOA model and other PV models is made in this study. GOA succeeds to build an accurate, reliable PV model that can be used in simulating and studying the PV system.

This work is arranged in its current form as follows: Section 2 explains PV module modeling. Section 3 discusses the problem formulation. In Section 4, the GOA is presented. Section 5 discusses in detail the simulation outcomes and its fair comparison with that achieved through the experimental tests. In Section 6, conclusions are inferred.

2. Mathematical Modeling of a PV Module

In this approach, the three-diode model is chosen to model the PV cell. The three diode model is shown in Figure 1. The three currents in the three diodes are I_{d1}, I_{d2}, I_{d3}. I_{d1} represents the current due to diffusion and recombination in the emitter and bulk regions of the P–N junction. I_{d2} is the recombination current in the depletion region. I_{d3} represents the effect of grain boundaries and leakage current. The series resistance (R_s) signifies the semiconductor material resistance at the neutral regions of the solar cell. The parallel resistance (R_p) is the leakage current at the surface of the solar cell [21].

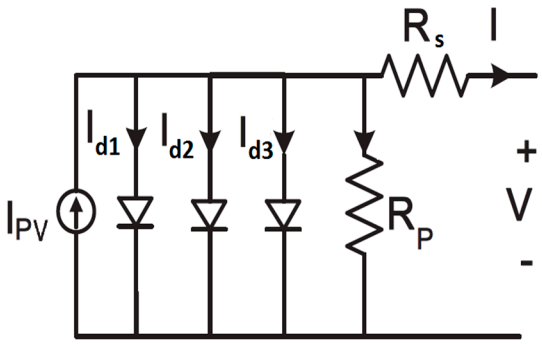

Figure 1. Three diode Photovoltaic (PV) model.

The current of such PV module is mathematically formulated as follows [20]:

$$I = I_{PV} - I_{o1}\left\{\exp\left[\frac{(V + IR_S)}{\alpha_1 V_{th}}\right] - 1\right\} - I_{o2}\left\{\exp\left[\frac{(V + IR_S)}{\alpha_2 V_{th}}\right] - 1\right\} - I_{o3}\left\{\exp\left[\frac{(V + IR_S)}{\alpha_3 V_{th}}\right] - 1\right\} - \frac{V + IR_S}{R_P} \quad (1)$$

where I_{PV} is the cell-generated photocurrent; I_{o1}, I_{o2}, and I_{o3} are the saturation currents of the three diodes; α_1, α_2, α_3 are the diode ideality factor for the three diodes; V_{th} is the PV module thermal voltage; I is the current of PV module. V is the PV module output voltage.

The values of some parameters change with the variation in temperature and irradiance. Thus, these variations are formulated in the following equations [37,38]:

$$I_{pv} = \left(I_{pvn} + k_i \Delta T\right)\frac{G}{G_n} \quad (2)$$

$$I_o = I_{on}\left(\frac{T}{T_n}\right)^3 e^{\left[\frac{q \times E_g}{\alpha \times k}\left(\frac{1}{T_n} - \frac{1}{T}\right)\right]} \quad (3)$$

$$E_g = E_{gn}(1 - 0.0002677\Delta T) \quad (4)$$

$$R_p = R_{pn}\frac{G}{G_n} \quad (5)$$

where I_{PV}, I_{on}, E_{gn}, G_n, R_{pn}, and T_n are considered photocurrent, the saturation current, material band gap, solar irradiation, circuit shunt resistance, and cell temperature at the standard test condition (STC), respectively. E_{gn} has a value of 1.121 eV for silicon cells [37], ΔT is the temperature difference between T and T_n. K_i is the coefficient of short-circuit current.

3. Formulation of The Optimization Problem

Estimation of PV cell model parameters problem is formulated as an objective function. The proper designation of the fitness function is very significant for accurate identification of unknown parameters. The extracted parameter values must guarantee that the model behaves exactly as the PV panel.

In this study, the target of the fitness function is to minimize the root mean square error between estimated model current and its practical values [36]. This fitness function is written by the following equation:

$$\varepsilon = \sqrt{\frac{1}{N}\sum_{k=1}^{N} f_k^2(V, I, \varnothing)} \tag{6}$$

where N of the last equation represents the number of experimental samples, $\emptyset$ represents the design variables vector such that $\emptyset = \{I_{PV}, I_{o1}, I_{o2}, I_{o3}, R_S, R_P, \alpha_1, \alpha_2, \alpha_3\}$; $f_k(V, I, \varnothing)$ is represented by the following equation:

$$f_k(V, I, \varnothing) = I_{PV} - I_{o1}\left\{\exp\left[\frac{(V + IR_S)}{\alpha_1 V_{th}}\right] - 1\right\} - I_{o2}\left\{\exp\left[\frac{(V + IR_S)}{\alpha_2 V_{th}}\right] - 1\right\} - I_{o3}\left\{\exp\left[\frac{(V + IR_S)}{\alpha_3 V_{th}}\right] - 1\right\} - \frac{V + IR_S}{R_P} - I \tag{7}$$

This study aims at optimizing Equation (7) with respect to $\emptyset$. The GOA is used to solve this objective function to obtain the unknown parameters of the three diode PV models.

4. GOA

The GOA is a recent swarm intelligence algorithm developed by Mirjalili and other researchers. The GOA is imitating the social behavior of grasshopper swarms. This algorithm is a population-based method. Grasshoppers pass through two phases of development in their life cycle beginning as nymphs then adults. The nymph grasshoppers are wingless, slowly herbivores. When they mature, adults grow wings and fly fast on a large-scale area. Grasshoppers gather to form one of the hugest known swarms. The distinctive feature in grasshoppers is that they exhibit the swarming behavior in the larval and adulthood phase. The larval phase is characterized by the slow motion and little steps of grasshoppers. While long-range and quick movement are the fundamental features of the swarm in adulthood. Another vital feature in the grasshoppers' swarming is the food source seeking. Grasshoppers naturally move abruptly and locally in small areas to search for food. This divides the search process into two main stages that represent exploration and exploitation.

Inspecting the swarm motion, there are three different forces that specifies the location of the grasshopper in the swarm. The position of each grasshopper specifies a possible solution in the population. The three forces on each grasshopper are the social interaction between it and the other grasshoppers (S_i), the gravitational force applied on it (G_i) and the wind advection (A_i). The total forces on each grasshopper is represented as follows:

$$X_i = r_1 S_i + r_2 G_i + r_3 A_i \tag{8}$$

where X_i is the position of ith grasshopper. r_1, r_2, r_3 are random variables. The social interaction force between each grasshopper and the other grasshopper can be defined as follows:

$$S_i = \sum_{\substack{j=1 \\ j \neq i}}^{N} s\,(d_{ij})\mathbf{d_{ij}} \tag{9}$$

where d_{ij} dictates the distance between the grasshopper i and j. $\mathbf{d_{ij}}$ is distance unit vector from the ith grasshopper to the jth grasshopper. s is a function that represents the strength of two social forces, attraction and repulsion, between grasshoppers, and it can be formulated as follows:

$$s(r) = fe^{\frac{-r}{l}} - e^{-r} \tag{10}$$

where f, l are the attraction intensity and the attractive length scale, respectively. The function s divides the search space into comfort, repulsion, and attraction zones; however, its ability decreases to zero when the distance between two grasshoppers is greater than 10. To avoid this problem, the distance between grasshoppers is mapped between 1 and 4. If the distance between two grasshoppers is between 0 and 2.079 then a repulsion force exhibits, but if it is greater than 2.079, attraction force appears but it diminishes gradually after it reaches 4. When the distance between two grasshoppers is 2.079, there will be a comfortable zone, where there is neither attraction nor repulsion.

The gravity force applied on each grasshopper is calculated as follows:

$$G_i = -g\mathbf{e_g} \tag{11}$$

where g indicates the gravitational constant and $\mathbf{e_g}$ is a center of earth unity vector.

The nymph grasshoppers' motion depends to a great extent on the wind direction as they lack wings. The direction of wind can be estimated as indicated:

$$A_i = u\mathbf{e_w} \tag{12}$$

where u refers to a constant drift and $\mathbf{e_w}$ is a wind direction unity vector.

The grasshopper position is calculated as follows:

$$X_i = \sum_{\substack{j=1 \\ j \neq i}}^{N} s\Big(\big|x_j - x_i\big|\Big)\frac{x_j - x_i}{d_{ij}} - g\mathbf{e_g} + u\mathbf{e_w} \tag{13}$$

This equation is reformulated as shown to avoid any fast arrival to the comfort zone that could lead to a local optimum solution:

$$X_i^d = c\left(\sum_{\substack{j=1 \\ j \neq i}}^{N} c\frac{ub_d - lb_d}{2} s\Big(\big|x_j^d - x_i^d\big|\Big)\frac{x_j - x_i}{d_{ij}}\right) + \mathbf{T_d} \tag{14}$$

where ub_d, lb_d are the higher and lower boundaries in the dth dimension. $\mathbf{T_d}$ is the target value in the dth dimension which is the best solution found so far. $\mathbf{T_d}$ simulates the tendency to move towards

the source of food. The parameter c is a decreasing coefficient that achieves balance between both the exploration and the exploitation procedures in the GOA and it can be estimated as shown:

$$c = c_{max} - l\frac{c_{max} - c_{min}}{L} \quad (15)$$

where c_{max}, c_{min} are the maximum and minimum values respectively, l is the current iteration and L is its maximum value. The pseudo code of the GOA is illustrated in Figure 2. The algorithm begins by setting the initial values of c_{max}, c_{min}, f, l and L. The first population is generated randomly. The value of each solution in the population is calculated by the fitness function, then the best solution is assigned. At the beginning of each new iteration, the coefficient parameter c is updated to shrink the three interaction zones as shown in Equation (15). Each solution in the population is updated as illustrated in Equation (14). If any of the updated solutions violate its lower and upper boundaries, it is returned to its position. The updated solutions are evaluated, and the best global solution is allocated. The overall operations are repeated until reaching to L which is the termination criterion in this algorithm and the best global solution T is returned.

Let the swarm $\mathbf{X_i}$ $(\mathbf{i} = \mathbf{1}, \mathbf{2}, \ldots \mathbf{n})$
Set c_{max}, c_{min} and L
Evaluate the fitness function for each particle
let O = the optimum search particle
while (l < L)

$$\mathbf{c} = \mathbf{c_{max}} - \mathbf{l}\frac{\mathbf{c_{max}} - \mathbf{c_{min}}}{\mathbf{L}}$$

for each particle

Normalize distance among grasshoppers

Update the location of the present particle

If the boundaries are exceeded, return the current search agent to its position.

End for

Update O if an optimum solution is found

l = l + 1

end while

Return O

Figure 2. Pseudo code of the Grasshopper Optimization Algorithm (GOA).

5. Simulation Results

In this research, KC200GT and MSX-60 polycrystalline PV modules are used to verify the validity of the GOA-based PV model. The specifications of the electrical performance of these commercial PV modules under the STC condition are illustrated in Table 1 [39,40]. Figure 3a,b points out the objective function convergence for both modules. The number of iterations set for every module is 1000 and the number of search agents is 60. The convergence speed is very high for each module. The best optimal value of the objective function found by GOA is 9.9775×10^{-11} and 7.592×10^{-10} for KC200GT and MSX-60 modules, respectively. The obtained results of the proposed GOA are compared with that obtained using the whale optimization algorithm (WOA), genetic algorithm (GA), Simulated Annealing technique (SA) for KC200GT PV modules in Table 2. To inspect the results of MSX-60 module, the fitness function is optimized with GA technique and SA technique using Optimization Toolbox embedded in MATLAB, the fitness function is also optimized using WOA and the results are compared with the GOA in Table 3. The values of the undetermined parameters of these PV models using the GOA are around the values obtained from other methods and are within an acceptable range. Figure 4a illustrates the I-V curves of the proposed GOA model and those for the practical data of the KC200GT PV module under various temperature conditions. Figure 4b shows the power versus voltage (P-V) curves of the GOA PV model and those for the practical data of the KC200GT PV module at various temperature conditions. It can be seen clearly that the I-V and P-V curves of the GOA PV model and those of practical data are matching. This demonstrates the great precision in the proposed PV model regardless of temperature variations. Figure 5a illustrates the I-V curves of the proposed GOA model and those for the practical data of the KC200GT PV module at various irradiations conditions. Figure 5b shows the P-V curves of the GOA model and the practical data of the KC200GT PV module at various irradiation conditions.

Table 1. Specification of PV Modules.

Parameters	KC200GT	MSX-60
I_{sc}	8.21 A	3.8 A
V_{oc}	32.9 V	21.1 V
I_{mp}	7.61 A	3.5 A
V_{mp}	26.3 V	17.1 V
P_{max}	200 W	60 W
K_v	−0.123 V/°C	−0.08 V/°C
K_i	0.00318 A/°C	0.00065 A/°C
N_s	54	36

Table 2. Comparison among Optimum models for KC200GT.

Method	GA [21]	SA	WOA [21]	GOA
I_{o1} (A)	1.52×10^{-8}	1.43×10^{-8}	2.692×10^{-8}	2.888514×10^{-8}
I_{o2} (A)	4.58×10^{-10}	4.26×10^{-10}	4.678×10^{-10}	2.802112×10^{-10}
I_{o3} (A)	1.019×10^{-10}	2.43×10^{-10}	4.927×10^{-10}	2.797361×10^{-10}
R_s (Ω)	0.3614	0.3207	0.34215	0.2248107
R_p (Ω)	311.8	289.6462	341.3875	310.8623
$\propto_1$	1.189	1.182898	1.32	1.219762
$\propto_2$	1.495	1.263977	1.236	1.091667
$\propto_3$	1.238	1.456052	1.0216	1.499932
I_{pv} (A)	8.143	8.12605	8.231	8.229174

Table 3. Comparison among Optimum models for MSX-60.

Method	GA	SA	WOA	GOA
I_{o1} (A)	1.29597×10^{-7}	3.2164×10^{-7}	2.44146×10^{-7}	2.18714×10^{-7}
I_{o2}(A)	3.19663×10^{-10}	1.8573×10^{-10}	1.873735×10^{-10}	2.294004×10^{-10}
I_{o3}(A)	3.09854×10^{-10}	1.0186×10^{-10}	4.64888×10^{-10}	2.210856×10^{-10}
R_s (Ω)	0.3067643	0.155045	0.1615253	0.1109557
R_p (Ω)	193.615	230.855	266.8166	349.8458
$\propto_1$	1.3759	1.3935	1.397359	1.375876
$\propto_2$	1.23815	1.4765	1.092094	1.074414
$\propto_3$	1.13	1.3795	1.413907	1.094849
I_{pv} (A)	3.5885	3.9825	3.7438	275.5264

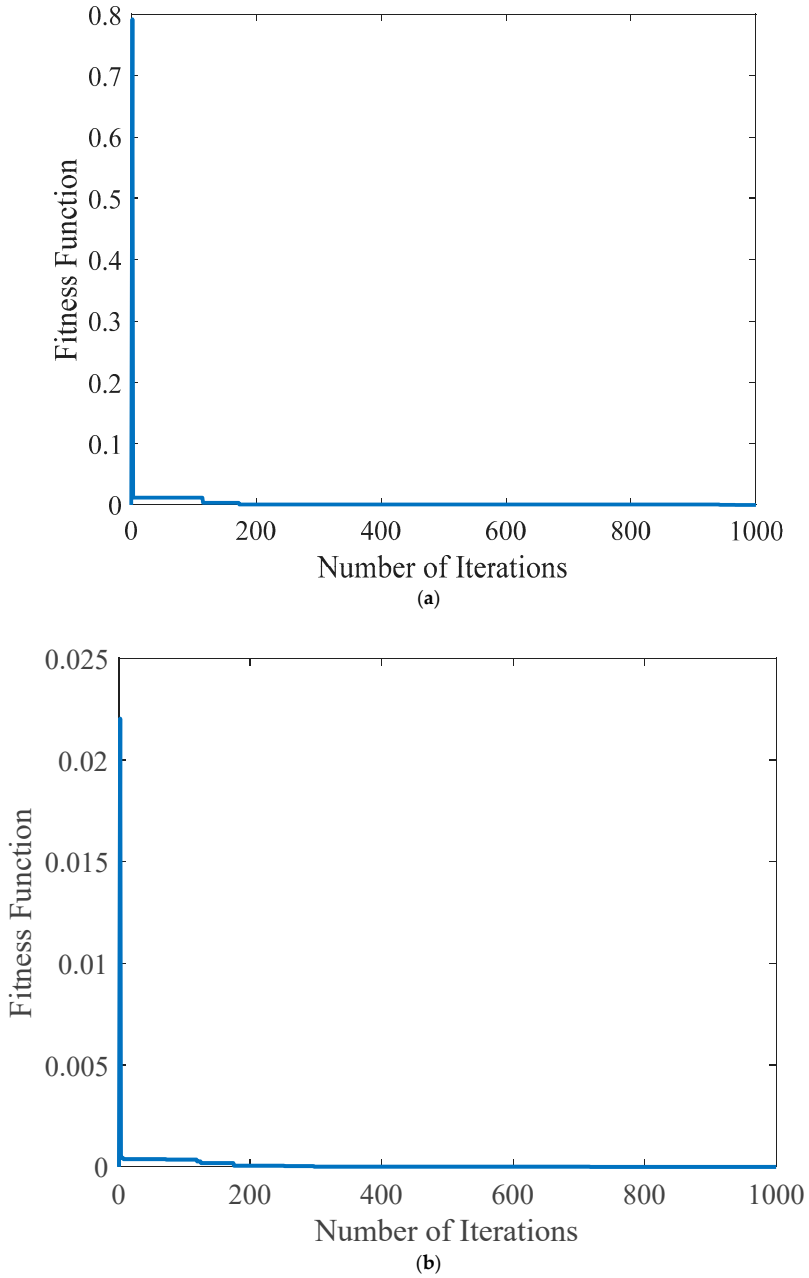

Figure 3. Objective function convergence. (**a**) KC200GT; (**b**) MSX60.

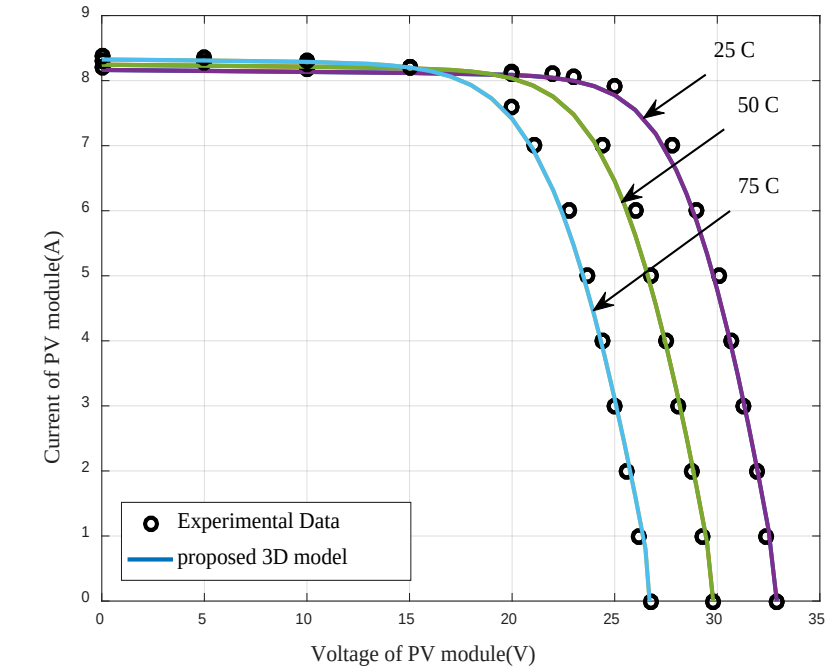

(**a**)

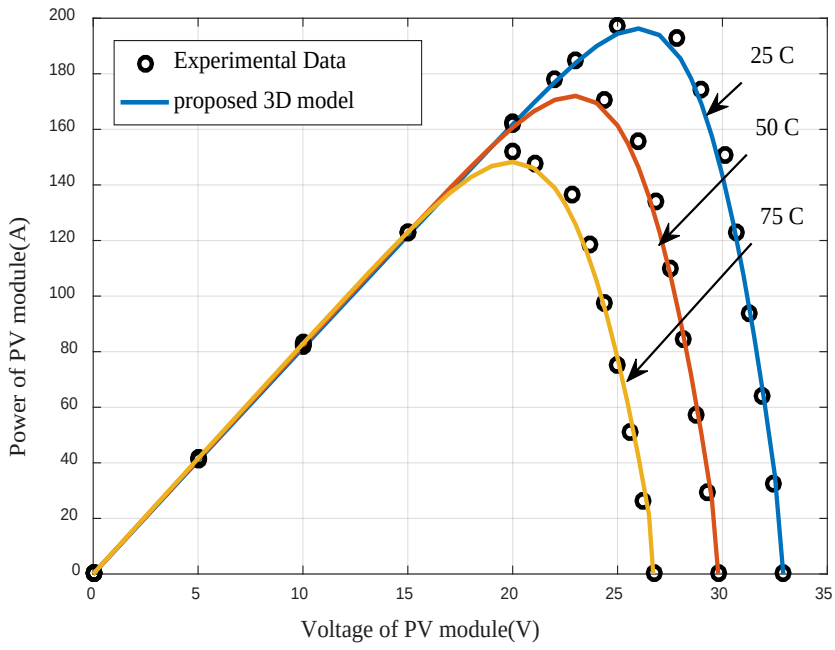

(**b**)

Figure 4. GOA-based simulation results and practical data of KC200GT module at various temperature conditions, G = 1000 W/m^2. (**a**) I-V curves; (**b**) P-V curves.

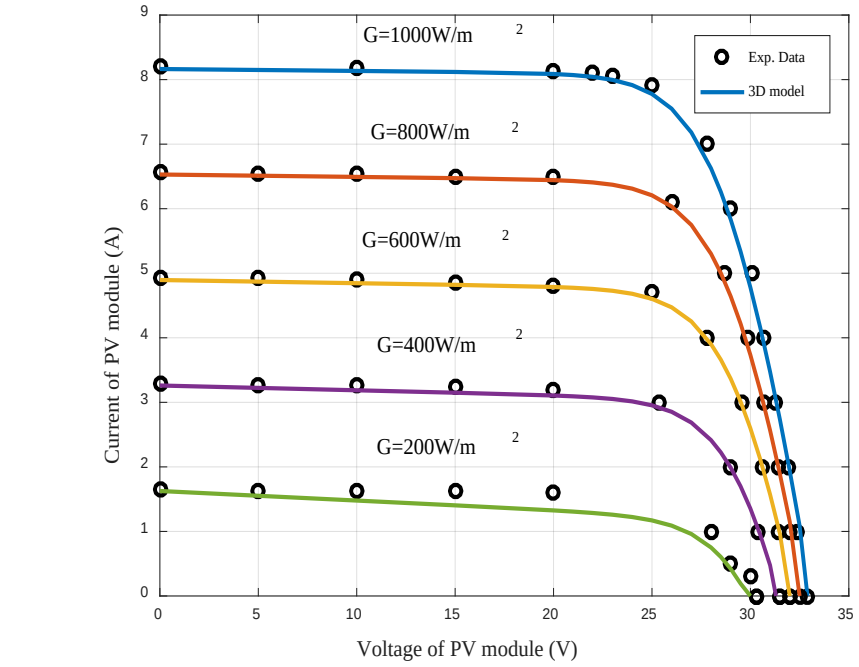

(**a**)

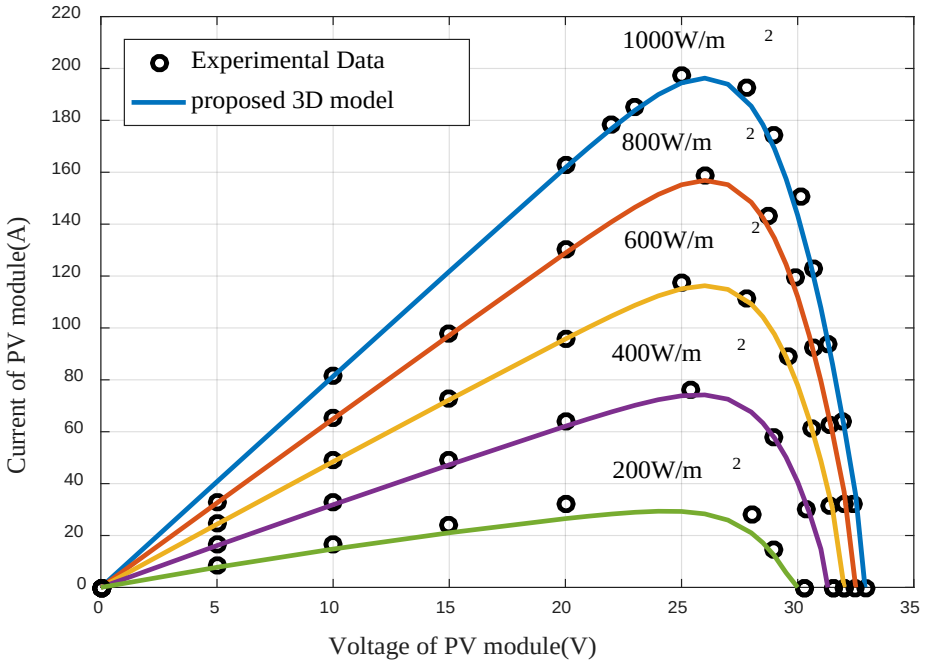

(**b**)

Figure 5. GOA-based simulation results and practical data of KC200GT module at various irradiation conditions, temperature = 25 °C (**a**) I-V curves; (**b**) P-V curves.

Figure 6a points out the I-V curves of the proposed GOA model and the practical data of the MSX-60 PV module at various temperature conditions. Figure 6b demonstrates the P-V curves of the proposed GOA model and the practical data of the MXS-60 PV module at various temperature conditions.

No deviations can be noticed between the simulation and experimental results. These graphical comparisons judge and verify the validity of the novel GOA PV model. Figure 7a,b shows another graphical comparison between the current errors for KC200GT and MSX-60 modules and the error of

other techniques. In case of KC200GT PV module, the current error of the GOA PV model is very small, and it shows better results than most of the introduced models except at a small portion on the curve. In case of MSX-60 PV module, the current error of the GOA PV model is less than that achieved by using other PV models. This reflects the proper design of the proposed GOA and its high performance to achieve good results.

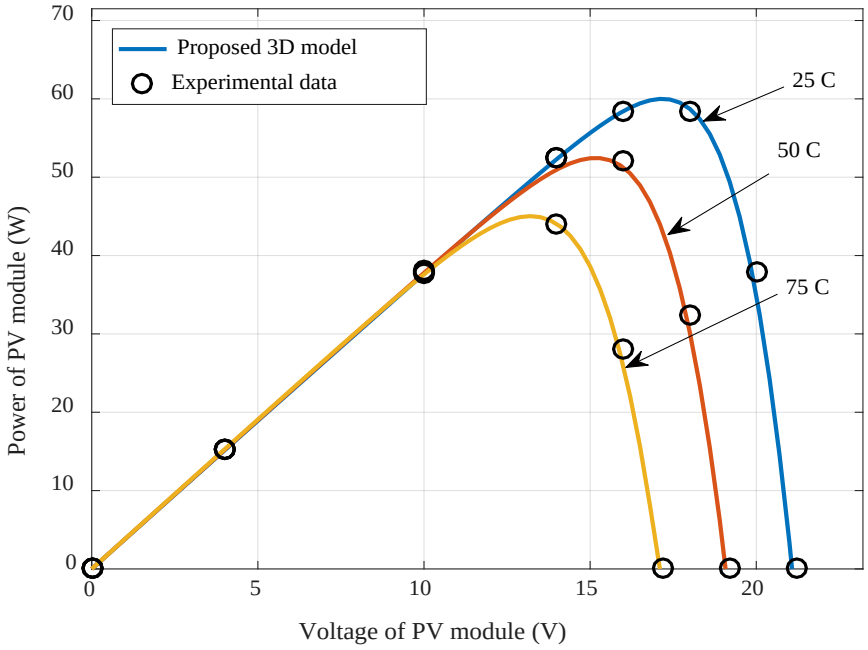

(**a**)

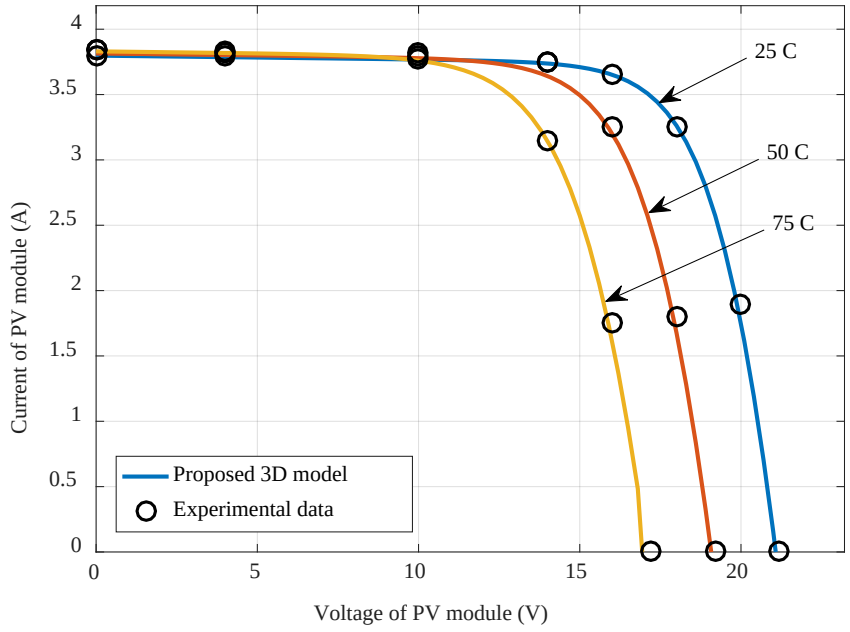

(**b**)

Figure 6. GOA-based simulation results and practical data of MSX-60 module at various temperature conditions, G = 1000 W/m^2. (**a**) I-V curves. (**b**) P-V curves.

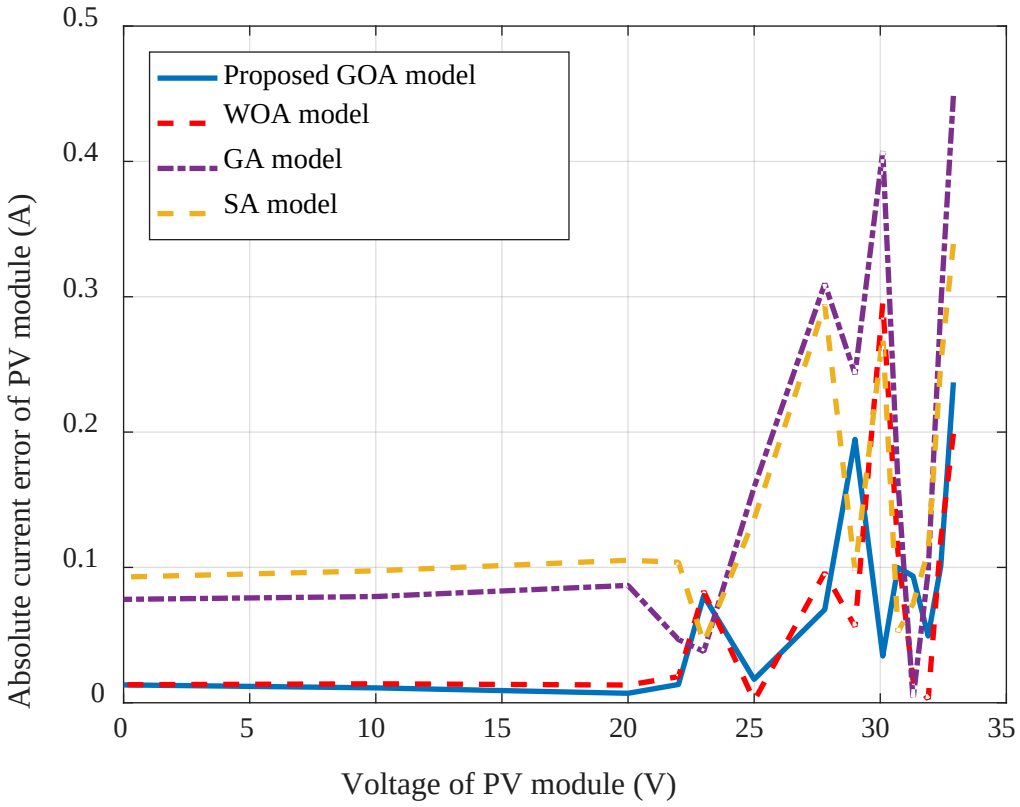

(**a**)

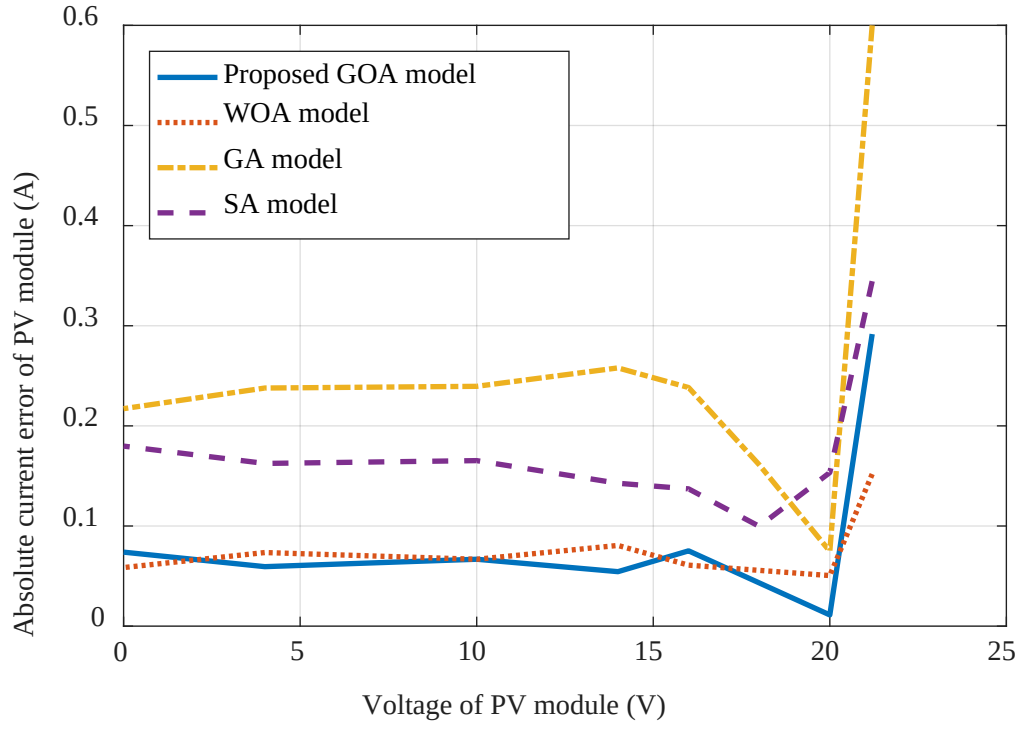

(**b**)

Figure 7. Absolute current error of the GOA-based PV model, MATLAB model, whale optimization algorithm (WOA) model, genetic algorithm (GA) model, and simulated annealing technique (SA) model. (**a**) KC200GT. (**b**) MSX-60.

6. Conclusions

In this paper, the GOA as a novel application to extract the undetermined parameters of the PV model of a PV module is exhibited. The problem formulation is based on minimizing the root mean-square error between calculated current and measured data by adjusting parameters of the proposed model. Simulation is carried out under different environmental conditions of temperature and irradiance level. The PV model results nearly coincide with its experimental results. The efficiency of the GOA PV model is tested by comparing the simulation results with the results of other optimization methods-based PV models. The results are within an acceptable range. The effectiveness of such model is evaluated by making a fair comparison among its current error and the current error of other PV models. The GOA has proved its superiority and high performance in case of KC200GT PV modules and MSX-60 PV modules. The GOA has succeeded in optimizing the parameters of the three-diode model. The proposed GOA may be extended to solve other optimization problems in several research fields such as wind energy systems, other renewable energy systems and smart grids.

Author Contributions: In this article, the authors have exerted sincere efforts to be a high quality paper. In this regard, O.S.E. and I.A. have worked on the simulation results. H.M.H. shares in writing the paper and the revisions. A.Y.A. and S.M.M. help in reviewing the paper. All authors have read and agreed to the published version of the manuscript.

Funding: This research received no external funding.

Conflicts of Interest: The authors declare that they have no potential conflict of interest should be reported.

References

1. Chen, X.; Du, Y.; Wen, H.; Jiang, L.; Xiao, W. Forecasting-based power ramp-rate control strategies for utility-scale PV systems. *IEEE Trans. Ind. Electron.* **2019**, *66*, 1862–1871. [CrossRef]
2. Jäger-Waldau, A. *JRC PV Status Report 2018*; Publications Office of the European Union: Luxembourg, 2018; ISBN 978-92-79-97465-6.
3. Global Market Outlook for Solar Power 2017/2021 by Solar Power Europe. Available online: http://www.solarpowereurope.org (accessed on 15 May 2017).
4. Keerthisinghe, C.; Chapman, A.C.; Verbic, G. PV and demand models for a Markov decision process formulation of the home energy management problem. *IEEE Trans. Ind. Electron.* **2019**, *66*, 1424–1433. [CrossRef]
5. Mathew, D.; Rani, C.; Kumar, M.R.; Wang, Y.; Binns, R.; Busawon, K. Wind-Driven Optimization Technique for Estimation of Solar Photovoltaic Parameters. *IEEE J. Photovolt.* **2018**, *8*, 248–256. [CrossRef]
6. Qais, M.H.; Hasanien, H.M.; Alghuwainem, S.; Nouh, A.S. Coyote optimization algorithm for parameters extraction of three-diode photovoltaic model of photovoltaic modules. *Energy* **2019**, *187*, 1–8. [CrossRef]
7. El-Naggar, K.M.; Alrashidi, M.R.; Alhajri, M.F.; Al-Othman, A.K. Simulated annealing algorithm for photovoltaic parameters identification. *Sol. Energy* **2012**, *86*, 266–274. [CrossRef]
8. Qais, M.H.; Hasanien, H.M.; Alghuwainem, S. Identification of electrical parameters for three-diode photovoltaic model using analytical and sunflower optimization algorithm. *Appl. Energy* **2019**, *250*, 109–117. [CrossRef]
9. Xiong, G.; Zhang, J.; Yuan, X.; Shi, D.; He, Y.; Yao, G. Parameter estimation of solar photovoltaic models by means of a hybrid differential evolution with whale optimization algorithm. *Solar. Energy* **2018**, *176*, 742–761. [CrossRef]
10. Gazi Islam, S.M.; Al-Durra, A.M.; Hasanien, H.M. RTDS implementation of an improved sliding mode based inverter controller for PV system. *ISA Trans.* **2016**, *62*, 50–59. [CrossRef]
11. Yu, K.; Liang, J.J.; Qu, B.Y.; Chen, X.; Wang, H. Parameters identification of photovoltaic models using an improved Jaya optimization algorithm. *Energy Conver. Manag.* **2017**, *150*, 742–753. [CrossRef]
12. Chin, V.J.; Salam, Z.; Ishaque, K. Cell modelling and model parameters estimation techniques for photovoltaic simulator application: A review. *Appl. Energy* **2015**, *154*, 500–519. [CrossRef]
13. Mahmoud, Y.; El-Saadany, E.F. A photovoltaic model with reduced computational time. *IEEE Trans. Ind. Electron.* **2015**, *62*, 3534–3544. [CrossRef]

14. Hasanien, H.M. Shuffled frog leaping algorithm for photovoltaic model identification. *IEEE Trans. Sustain. Energy* **2015**, *6*, 509–515. [CrossRef]
15. AlHajri, M.F.; El-Naggar, K.M.; AlRashidi, M.R.; Al-Othman, A.K. Optimal extraction of solar cell parameters using pattern search. *Renew. Energy* **2012**, *44*, 238–245. [CrossRef]
16. Lim, H.I.; Ye, Z.; Ye, J.; Yang, D.; Du, H. A linear identification of diode models from single I–V characteristics of PV panels. *IEEE Trans. Ind. Electron.* **2015**, *62*, 4181–4193. [CrossRef]
17. Shannan, N.M.A.A.; Yahaya, N.Z.; Singh, B. Single-diode model and two-diode model of PV modules: A comparison. In Proceedings of the 2013 IEEE International Conference on Control System, Computing and Engineering, Mindeb, Malaysia, 29 November–1 Decemebr 2013; pp. 210–214.
18. Gupta, S.; Tiwari, H.; Fozdar, M.; Chandna, V. Development of a two diode model for photovoltaic modules suitable for use in simulation studies. In Proceedings of the 2012 Asia-Pacific Power and Energy Engineering Conference, Shanghai, China, 27–29 March 2012; pp. 1–4.
19. Kassis, A.; Saad, M. Analysis of multi-crystalline silicon solar cells at low illumination levels using a modified two-diode model. *Sol. Energy Mater. Sol. Cells* **2010**, *94*, 2108–2112. [CrossRef]
20. Nishioka, K.; Sakitani, N.; Uraoka, Y.; Fuyuki, T. Analysis of multicrystalline silicon solar cells by modified 3-diode equivalent circuit model taking leakage current through periphery into consideration. *Sol. Energy Mater. Sol. Cells* **2007**, *91*, 1222–1227. [CrossRef]
21. Omnia, S.; Elazab, H.M.; Hasanien, M.A.E.; Abdeen, A.M. Parameters estimation of single- and multiple-diode photovoltaic model using whale optimisation algorithm. *IET Renew. Power Gener.* **2018**, *12*, 1755–1761.
22. Ghani, F.; Duke, M.; Carsona, J. Numerical calculation of series and shunt resistance of a photovoltaic cell using the Lambert W-function: Experimental evaluation. *Sol. Energy* **2013**, *87*, 246–253. [CrossRef]
23. Jacob, B.; Balasubramanian, K.; Babu, T.S.; Rajasekar, N. Parameter extraction of solar PV double diode model using artificial immune system. In Proceedings of the IEEE International Conference on Signal Processing, Informatics, Communication and Energy Systems (SPICES), Kozhikode, India, 19–21 February 2015.
24. Mahmoud, Y.A.; Xiao, W.; Zeineldin, H.H. A simple approach to modeling and simulation of photovoltaic modules. *IEEE Trans. Sustain. Energy* **2012**, *3*, 185–186. [CrossRef]
25. Subudhi, B.; Pradhan, R. A comparative study on parameter estimation methods. *Int. J. Renew. Energy Technol.* **2012**, *3*, 295–315. [CrossRef]
26. Ishaque, K.; Salam, Z.; Taheri, H. Simple, fast and accurate two-diode model for photovoltaic modules. *Sol. Energy Mater. Sol. Cells* **2011**, *95*, 586–594. [CrossRef]
27. Gow, J.A.; Manning, C.D. Development of a photovoltaic array model for use in power-electronics simulation studies. *IEE Proc. Electr. Power Appl.* **1999**, *146*, 193–200. [CrossRef]
28. Sandrolini, L.; Artioli, M.; Reggiani, U. Numerical method for the extraction of photovoltaic module double-diode model parameters through cluster analysis. *Appl. Energy* **2010**, *87*, 442–451. [CrossRef]
29. Spall, J.C. An overview of the simultaneous perturbation method for efficient optimization. *Johns Hopkins APL Tech. Dig.* **1998**, *19*, 482–493.
30. Yao, X.; Liu, Y.; Lin, G. Evolutionary programming made faster. *IEEE Trans. Evol. Comput.* **1999**, *3*, 82–102.
31. Benkercha, R.; Moulahoum, S.; Colak, I.; Taghezouit, B. PV module parameters extraction with maximum power point estimation based on flower pollination algorithm. In Proceedings of the IEEE International Power Electronics and Motion Control Conference (PEMC), Varna, Bulgaria, 25–28 September 2016.
32. Saremi, S.; Mirjalili, S.; Lewis, A. Grasshopper optimisation algorithm: Theory and application. *Adv. Eng. Softw.* **2017**, *105*, 30–47. [CrossRef]
33. Łukasik, S.; Kowalski, P.A.; Charytanowicz, M.; Kulczycki, P. Data clustering with grasshopper optimization algorithm. In Proceedings of the Federated Conference on Computer Science and Information Systems, Prague, Czech Republic, 3–6 September 2017.
34. Wu, J.; Wang, H.; Li, N.; Yao, P.; Huang, Y.; Su, Z.; Yu, Y. Distributed trajectory optimization for multiple solar-powered UAVs target tracking in urban environment by Adaptive Grasshopper Optimization Algorithm. *Elsevier BV* **2017**, *70*, 497–510. [CrossRef]
35. Hekimoğlu, B.; Ekinci, S. Grasshopper optimization algorithm for automatic voltage regulator system. In Proceedings of the 2018 5th International Conference on Electrical and Electronic Engineering (ICEEE), Istanbul, Turkey, 3–5 May 2018; pp. 152–156.
36. Ishaque, K.; Salam, Z.; Mekhilef, S.; Shamsudin, A. Parameter extraction of solar photovoltaic modules using penalty-based differential evolution. *Appl. Energy* **2012**, *99*, 297–308. [CrossRef]

37. De Soto, W.; Klein, S.; Beckman, W. Improvement and validation of a model for photovoltaic array performance. *Sol. Energy* **2006**, *80*, 78–88. [CrossRef]
38. Sera, D.; Teodorescu, R.; Rodriguez, P. PV panel model based on datasheet values. In Proceedings of the 2007 IEEE International Symposium on Industrial Electronics, Vigo, Spain, 4–7 June 2007; pp. 2392–2396.
39. KC200GT High Efficiency Multicrystalline Photovoltaic Module Datasheet. Kyocera. Available online: http://www.kyocera.com.sg/products/solar/pdf/kc200gt.pdf (accessed on 10 February 2013).
40. MSX-60 Polycrystalline Silicon Photovoltaic Module Datasheet. Solar Electric Supply, Inc. Available online: http://www.solarelectricsupply.com/solar-panels/solarex/solarex-msx-60-w-junction-box (accessed on 20 March 2010).